Journal of Materials Chemistry: A. Volume 7, Issue 37, October 2019, pp. 20969–21526
DOI: 10.1039/C9TA04513A

A Facile One-Pot Synthesis of CaO/CuO Hollow Microspheres Featuring Highly Porous Shells for Enhanced CO_2 Capture in Combined Ca-Cu Looping Process via a Template-Free Synthesis Approach

Jian Chen,[†,‡] Lunbo Duan,[†] Tian Shi,[†] Ruoyu Bian,[†] Yuxiao Lu,[†] Felix Donat,[‡] Edward J. Anthony[§]*

[†] Key Laboratory of Energy Thermal Conversion and Control, Ministry of Education, School of Energy and Environment, Southeast University, Nanjing 210096, China;

[‡] Laboratory of Energy Science and Engineering, ETH Zürich, Leonhardstrasse 21, 8092 Zürich, Switzerland;

[§] School of Power Engineering, Cranfield University, Cranfield, Bedfordshire MK43 0AL, United Kingdom.

ABSTRACT: The preparation of bifunctional CaO/CuO composites with high performance is essential for the development of the combined Ca-Cu looping process, in which the exothermic reduction of CuO with methane is used in-situ to provide the heat required to calcine $CaCO_3$. However, the rapid decline in CO_2 uptake of CaO/CuO composites remains an important problem

to be solved, despite their excellent redox characteristic. Herein we report a facile one-pot template-free synthesis approach to yield CaO/CuO hollow microspheres, aimed at enhancing the CO_2 capture performance of CaO/CuO composites. CaO/CuO hollow microspheres feature highly porous shells and a homogeneous elemental distribution, and demonstrate significantly enhanced CO_2 capture performance. After ten repeated cycles, CO_2 uptake capacity of the best-performing CaO/CuO hollow microspheres exceeded the reference materials, i.e., CaO/CuO composites synthesized via wet mixing or a co-precipitation method, by 222% and 114%, respectively. Moreover, from cycle number eight onwards, the CO_2 uptake was very stable over the tested 20 cycles, suggesting good cyclic stability of CaO/CuO hollow microspheres. Oxidation was always fast with conversions greater than 90%. On the basis of N_2 adsorption, scanning electron microscopy (SEM) and transmission electron microscopy (TEM) characterizations, the significantly enhanced CO_2 capture performance of the CaO/CuO hollow microspheres resulted from the unique hollow microsphere structure with highly porous shells, which remained throughout the cyclic operations.

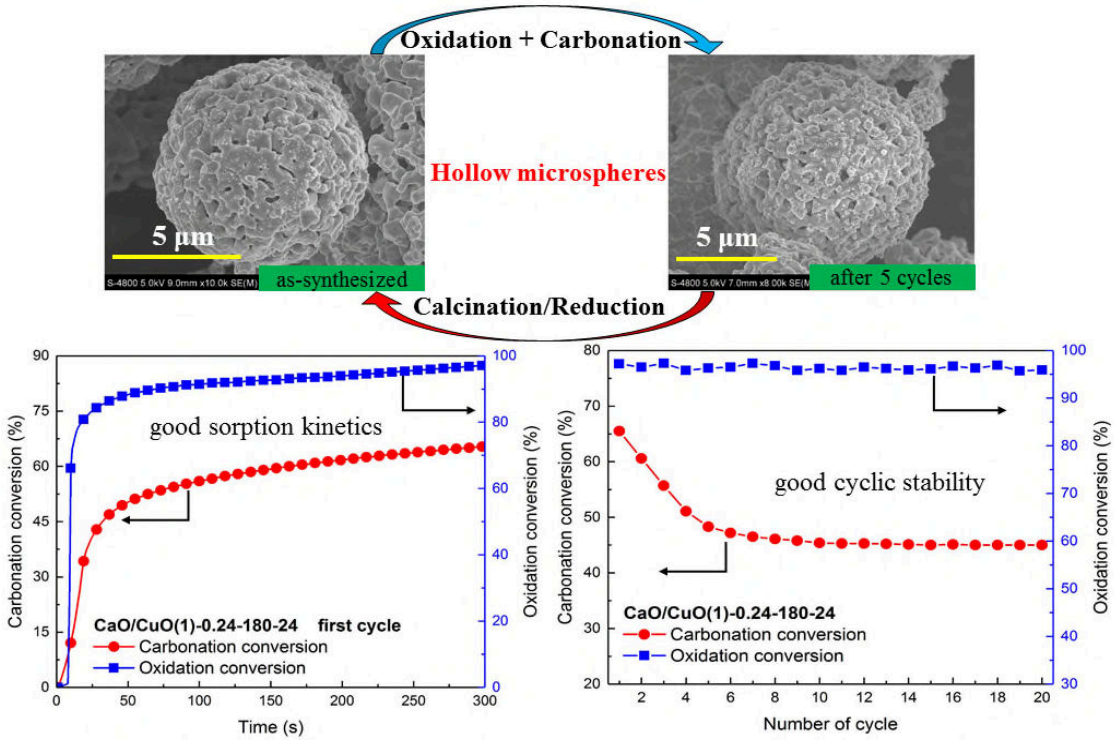

INTRODUCTION

The combined Ca-Cu looping process, a modification of conventional calcium looping (CaL) for CO_2 capture through CaO-based sorbents,[1-6] has been proposed recently to reduce the energy requirements for sorbent regeneration.[7-10] In this novel process, chemical looping combustion is integrated into the conventional CaL process by means of bifunctional CaO/CuO composites, where CaO functions as a sorbent for CO_2 capture and CuO functions as an oxygen carrier. The heat required for the regeneration of $CaCO_3$ is provided in-situ by the exothermic reaction between CuO and a reducing gaseous fuel,[11] as illustrated in Figure 1. Implementation of an energy-intensive air separation unit (ASU) can be avoided, which is otherwise necessary to produce pure oxygen for the oxy-fuel combustion in the calcination reactor to obtain a concentrated CO_2 stream.[12] A significantly reduced energy penalty (i.e., a drop in net power efficiency of the power

plant when carbon capture and sequestration (CCS) technology is used) of 3.4% can be obtained for the combined Ca-Cu looping process compared to an energy penalty of 7.9% for the conventional CaL configuration.[13] In addition to its application in the post-combustion CO_2 capture system, the combined Ca-Cu looping process can also be used for hydrogen production,[7] thus offering great potential in integration with other state-of-the-art technologies, such as hydrogen plants,[14-17] ammonia production plants,[18] natural gas combined cycle power plants,[19] steelworks,[20,21] and solid-oxide fuel cells.[22]

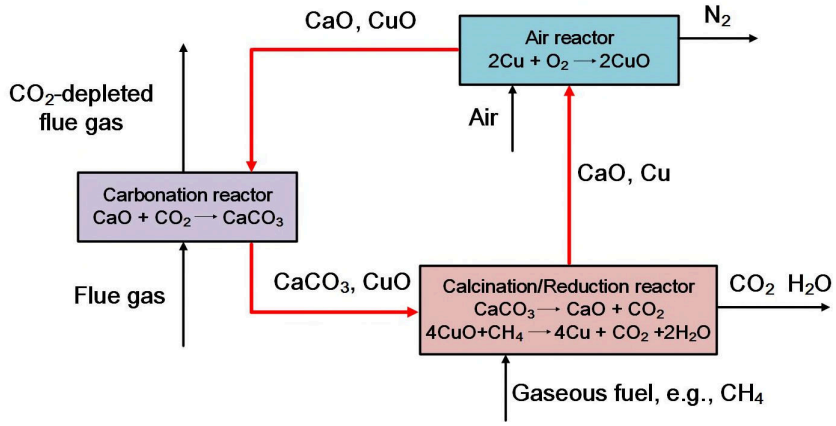

Figure 1. Schematic diagram of combined Ca-Cu looping process.

Although exhibiting vast application prospects as mentioned above, the combined Ca-Cu looping process is very challenging from a material point of view. Thus, although CaO/CuO composites exhibit excellent, cyclically stable O_2 carrying capacity, mainly due to CaO acting as a support for the CuO, the CO_2 uptake declines significantly during the cyclic operations and thus becomes a major problem to be solved.[23-26] For example, CaO/CuO composites prepared by a wet granulation approach possessed a carbonation conversion of 30% after only three cycles, in spite of using a thermally stable cement-type support.[27] In our recent work, we fabricated nanostructured CaO/CuO composites using a solution combustion synthesis method, and observed that the CO_2

uptake increased with an increase of cycle numbers; this has been termed self-activation.[23] However, the initial carbonation conversions were relatively low (less than 40%) and still need to be improved.

Recently, three-dimensional hierarchical hollow microspheres have attracted great interest in both fundamental and applied research, due to their well-defined morphologies, large surface areas and high performance for catalysis.[28-33] The most widely employed method for the production of hollow microsphere materials is the template-assisted synthesis approach using hard templates[34] such as mono-dispersed polymers,[35] carbonaceous spheres,[36] or carbon.[37] In general, this approach involves four major steps: 1) template preparation; 2) surface modification of the hard template; 3) target material coating/deposition; and 4) template removal.[34] Ma et al.,[38] Armutlulu et al.[39] and our group[36] successfully developed CaO hollow microspheres using this synthesis method, respectively, and confirmed the superiority of hollow microsphere structures for enhanced CO_2 capture performance of CaO-based sorbents. However, in order to limit the complexity and to increase the throughput of the synthesis procedure, a favorable approach should not involve the use of any templates, as they must be first prepared and then finally removed.

Here, we report a facile template-free synthesis approach to yield effective CaO/CuO hollow microspheres featuring highly porous shells and a homogeneous elemental distribution without any support material. The synthesis approach adopted here features the aforementioned desirable one-pot characteristics. The initial and cyclic carbonation and redox characteristics were assessed in detail and were also compared with CaO/CuO composites prepared by conventional synthesis methods, i.e., wet mixing and co-precipitation. N_2 adsorption, scanning electron microscopy (SEM) and transmission electron microscopy (TEM) confirmed the hollow microsphere structure

and the highly porous shells, which are essential to enhance the CO_2 capture performance of CaO/CuO composites.

EXPERIMENTAL SECTION

Materials and sorbent preparation. All the reagents used in the experiments were of analytical grade and employed without further purification. In a typical synthesis, calcium nitrate tetrahydrate ($Ca(NO_3)_2 \cdot 4H_2O$, 0.03 mol), cupric nitrate trihydrate ($Cu(NO_3)_2 \cdot 3H_2O$, 0.03 mol), and glycine ($C_2H_5NO_2$, 0.06 mol) were first dissolved in 125 mL of deionized water, as shown in Figure 2. After vigorous stirring for 5 min at room temperature, ammonium bicarbonate (NH_4HCO_3, 0.15 mol) was added slowly to the mixed solution. A solid-liquid mixture was obtained after the dissolution of NH_4HCO_3, which was then transferred into a 250 mL Teflon-lined stainless-steel autoclave. The autoclave was kept in an oven at 180 °C for 24 h. After cooling down to room temperature, a black powdery material was collected by centrifugation and filtration, and washed thoroughly with deionized water three times. The filtrate was dried in an oven at 120 °C for 12 h to remove water. The final CaO/CuO hollow microspheres were produced via calcination in a muffle furnace at 800 °C for 1 h with a slow heating rate (i.e., 2 °C/min from room temperature to 800 °C) under an air atmosphere. For comparison, samples with the same Ca/Cu molar ratio were also prepared by simple wet mixing of $Ca(NO_3)_2 \cdot 4H_2O$ and $Cu(NO_3)_2 \cdot 3H_2O$, as well as co-precipitation of $Ca(NO_3)_2 \cdot 4H_2O$ and $Cu(NO_3)_2 \cdot 3H_2O$ using NH_4HCO_3 as the precipitant, respectively. These reference materials also received the same calcination treatment.

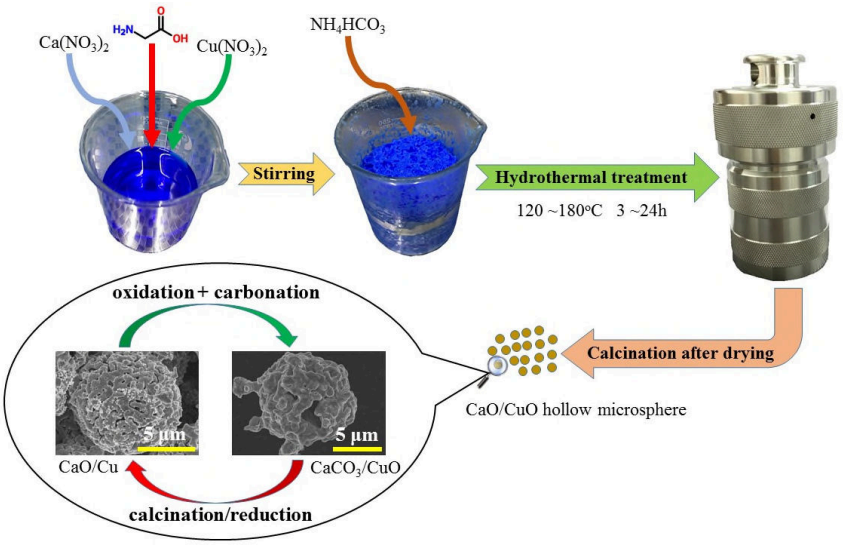

Figure 2. Schematic illustration of the facile template-free synthesis approach developed here to synthesize CaO/CuO hollow microspheres.

In this work, twelve CaO/CuO composites were synthesized and investigated. For simplicity, the abbreviation CaO/CuO(x)-y-T-t is used to denote the different CaO/CuO composites prepared by the template-free synthesis approach, where x represents the molar ratio of CaO to CuO, y is the molar concentration of Ca^{2+} precursor (mol/L), T is the hydrothermal temperature (°C), and t is the hydrothermal duration (h). Here, the abbreviations CaO/CuO(x)-y-WM and CaO/CuO(x)-y-CP are also used for CaO/CuO composites fabricated by wet mixing and co-precipitation methods, respectively. Table S1 in the Supporting Information (SI) summarizes all materials synthesized. Note that the molar ratio of CaO to CuO (i.e., x) in the composites investigated in this work was always one, although the theoretical ratio from balancing the reaction heats of the calcination of $CaCO_3$ (Eq. 1) and the reduction of CuO with CH_4 (Eq. 2) is ~0.25 and thus much lower. This is because the practically relevant molar ratio of CaO to CuO in the composites does not only depend on the reaction heats, but also on the extent of the carbonation reaction of CaO, which is usually incomplete and so unreacted CaO exists after each carbonation reaction. When thermal sintering

occurs, the CO_2 uptake capacity decreases even further and so does the heat requirement to decompose the carbonate.

$$CaCO_3 \leftrightarrow CaO + CO_2 \quad \Delta H_{298K} = +178 kJ \cdot mol^{-1} \tag{1}$$

$$CH_4 + 4CuO \rightarrow 4Cu + CO_2 + 2H_2O \quad \Delta H_{298K} = -170 kJ \cdot mol^{-1} \tag{2}$$

Detailed information concerning the experimental characterization and performance testing can be found in the SI. A schematic illustration of the fixed-bed reactor is shown in the SI, Figure S1.

RESULTS AND DISCUSSION

Synthesis of CaO/CuO hollow microspheres. It is well known that the carbonation reaction consists of two stages: an initial rapid kinetically-controlled stage, followed by a substantially slower diffusion-controlled stage.[41-43] Considering the typically short residence time in fixed-bed reactors, only the CO_2 captured during the kinetically-controlled stage is of practical relevance. As shown in Figure 3, compared to CaO/CuO composites prepared by conventional synthesis methods, such as wet mixing or co-precipitation, CaO/CuO hollow microspheres featuring highly porous shells provide a larger specific surface area with numerous active sites for the occurrence of the carbonation reaction, thus enabling rapid kinetics and a high sorption capacity. The central void provides the required volume to buffer against the volume variations accompanied with the repeated cyclic operations (i.e., carbonation/calcination of CaO/$CaCO_3$ and reduction/oxidation of CuO/Cu, as the molar volume of $CaCO_3$ is more than twice as high as that of CaO, and the molar volume of CuO is 1.7 times as high as that of Cu), thus leading to an improved cycling stability. This advantage was experimentally confirmed by Naeem et al.,[44] who used in-situ TEM to observe the morphological changes of CaO hollow microspheres during the calcination reaction, and found although the molar volume of $CaCO_3$ is more than twice as high as that of CaO, the shrinkage in

the diameter of the microsphere after calcination was determined to be <15%, which was due to the presence of the central void within the multi-shell architecture. Moreover, the presence of highly porous shells would allow rapid transport of CO_2 to and from the material.[39,45,46] It should also be noted that the shells are composed of CaO and CuO (or CaO, CuO and calcium copper oxide) nano-sized particles, among which CaO nanoparticles minimize the diffusion distance of CO_2 through the freshly formed $CaCO_3$ product layer in the diffusion-controlled stage during the carbonation reaction.[44] Furthermore, the three-dimensional hollow microsphere structures realize a physical separation of the nanoparticles, which is expected to effectively mitigate particle/grain agglomeration.[47]

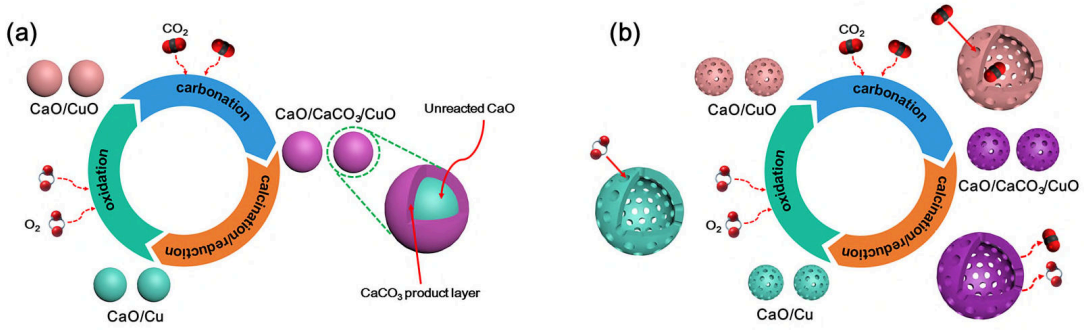

Figure 3. Microstructure modification to enhance CO_2 capture performance of CaO/CuO composites. (a) Assembly of relatively large CaO/CuO nanoparticles (i.e., prepared by the conventional synthesis methods) which suffers from diffusion-limited CO_2 uptake; (b) CaO/CuO hollow microspheres with highly porous shells.

In order to obtain the optimal synthesis parameters, their effects, such as concentration of calcium and copper precursors, hydrothermal duration and hydrothermal temperature, on the microstructures of CaO/CuO composites, were investigated in detail. Figure 4 shows the SEM images of CaO/CuO composites synthesized under different hydrothermal conditions. When the

157 molar concentration of Ca^{2+} was 0.04 mol/L, CaO/CuO composites showed irregular
158 morphologies, where CaO and CuO grains were connected with each other and agglomerated
159 (Figure 4a). The agglomeration of CaO and CuO grains became more severe as the molar
160 concentration of Ca^{2+} was increased to 0.08 mol/L; however, a fraction of CaO/CuO composites
161 exhibited morphologies of approximate microspheres (Figure 4b). With the continuous increase of
162 the molar concentration of Ca^{2+} to 0.24 mol/L, CaO/CuO composites yielded microsphere
163 morphologies featuring highly porous shells (Figure 4c, d). Figure 5 shows a typical STEM image
164 of CaO/CuO(1)-0.24-180-24 (i.e., a material that was synthesized at a hydrothermal temperature
165 of 180 °C for a hydrothermal duration of 24 h), which confirmed the hollow interiors clearly by
166 the electron-density difference between the dark edge and the pale center. Moreover, the particle
167 size and the shell thickness of CaO/CuO hollow microspheres became larger when the molar
168 concentration of Ca^{2+} was greater than 0.24 mol/L (Figure 4e, f, Figure 5 and SI, Figure S2).

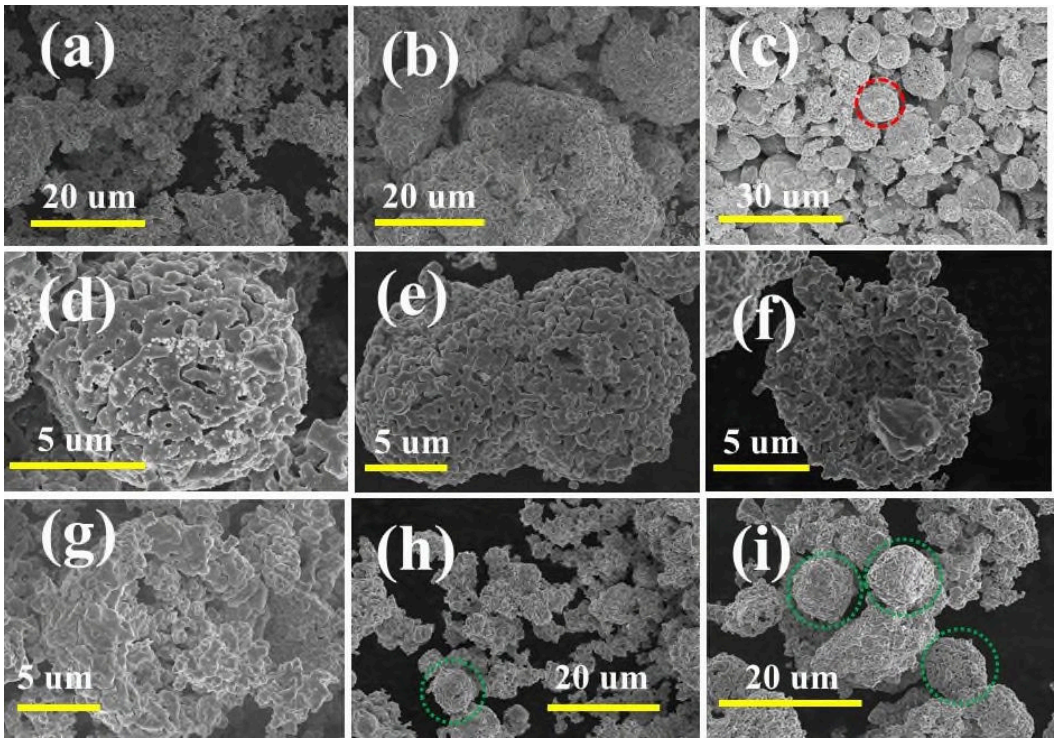

169

Figure 4. SEM images of CaO/CuO composites synthesized under different hydrothermal conditions. (a) CaO/CuO(1)-0.04-180-24; (b) CaO/CuO(1)-0.08-180-24; (c) CaO/CuO(1)-0.24-180-24; (d) high resolution of the red marked area in (c); (e), (f) CaO/CuO(1)-0.4-180-24; (g) CaO/CuO(1)-0.24-180-6; (h) CaO/CuO(1)-0.24-180-12; (i) CaO/CuO(1)-0.24-180-18. The green dotted circles indicate the presence of microspheres.

In addition, when the hydrothermal duration was 6 h, there were no CaO/CuO hollow microspheres formed, as shown in Figure 4g. However, CaO/CuO hollow microspheres were present once the hydrothermal duration was increased to 12 h (Figure 4h). The number of CaO/CuO hollow microspheres increased further as the hydrothermal duration was increased (Figure 4c, i). Furthermore, it was found that hydrothermal treatment, the presence of glycine, as well as a high hydrothermal temperature, were essential for the hollow microsphere structure development. Without hydrothermal treatment, CaO/CuO composites exhibited irregular morphologies, rather than microsphere morphologies (SI, Figure S3). Similar observations were also made in the absence of glycine (SI, Figure S4) or at a low hydrothermal temperature of 120 °C (SI, Figure S5).

Consequently, with the accurate control of the aforementioned synthesis parameters, it is relatively simple to scale up this synthesis approach to prepare CaO/CuO hollow microspheres featuring highly porous shells. Moreover, it is also noteworthy that, compared to chemical compounds used in conventional template-assisted synthesis approaches for the development of hollow-structured materials, such as carbonaceous spheres,[36] sulfonated polystyrene,[48] resorcinol and formaldehyde,[49] all of the precursors utilized in this template-free synthesis approach were relatively inexpensive and environmentally benign.

Characterization of CaO/CuO hollow microspheres. To evaluate the homogeneous elemental distribution of CaO and CuO in the CaO/CuO hollow microspheres, a feature that is critical to ensure excellent heat and mass transfer during the repeated calcination/reduction, oxidation and carbonation cycles, HAADF-STEM with EDX analyses, as well as SEM with EDX analyses, were conducted. Figure 5 and SI, Figure S6 show the elemental mappings of Ca, Mg and O of a CaO/CuO hollow microsphere, respectively. Both figures confirm that Ca and Cu elements were dispersed homogeneously either on the surface or within the structure of the hollow microspheres, revealing that the template-free synthesis approach ensured the compositional homogeneity between CaO and CuO in the CaO/CuO hollow microspheres.

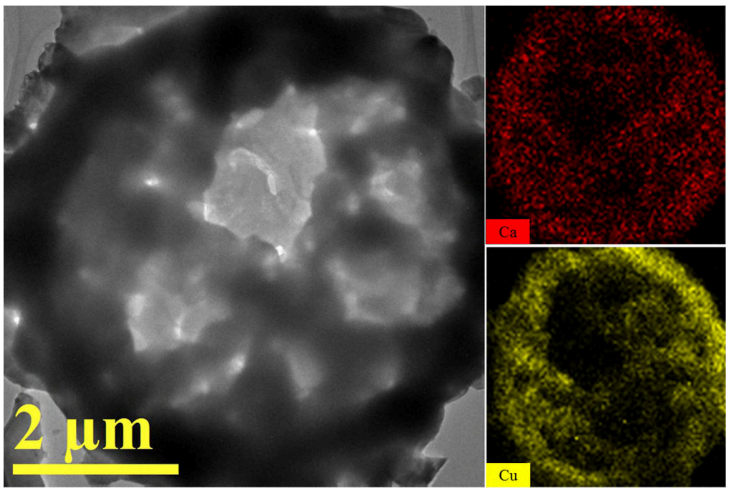

Figure 5. HAADF-STEM and EDX characterization of CaO/CuO(1)-0.24-180-24.

Figure 6 shows XRD diffractograms of CaO/CuO composites prepared by the template-free synthesis approach under different hydrothermal conditions. It was interesting to find that the main components of CaO/CuO(1)-0.24-180-6 and CaO/CuO(1)-0.24-180-12 were Ca_2CuO_3 and CuO. However, with the increase of hydrothermal duration, along with Ca_2CuO_3 and CuO, CaO was also detected. Although Ca_2CuO_3, a solid solution of CaO and CuO, has been commonly reported

in CaO-CuO pseudo-binary systems,[50,51] Ca_2CuO_3 present in CaO/CuO composites does not consume any "active CaO" and would subsequently decompose into CaO and CuO during the calcination/reduction stage. This conclusion was experimentally confirmed by Chen et al.,[23] who observed the phase evolution of CaO/CuO composites during the entire process (i.e., repeated calcination/reduction, oxidation and carbonation cycles) using in-situ XRD. Moreover, it seemed the concentration of the calcium precursor and the hydrothermal temperature had negligible effects on the composition of the CaO/CuO composites when the hydrothermal duration was as long as 24 h. The main components of the composites were always CaO, Ca_2CuO_3 and CuO. The presence of $Ca(OH)_2$ in CaO/CuO(1)-0.24-120-24 was probably due to adsorbed moisture (as shown in Eq. 3) when the sample was transferred to the XRD measurement. The calcination temperature used in the material synthesis process (i.e., 800 °C) was high enough for complete decomposition of $Ca(OH)_2$ (~550 °C),[52] even if $Ca(OH)_2$ did exist in the synthesis process before the calcination step.

$$CaO+H_2O \leftrightarrow Ca(OH)_2 \quad (3)$$

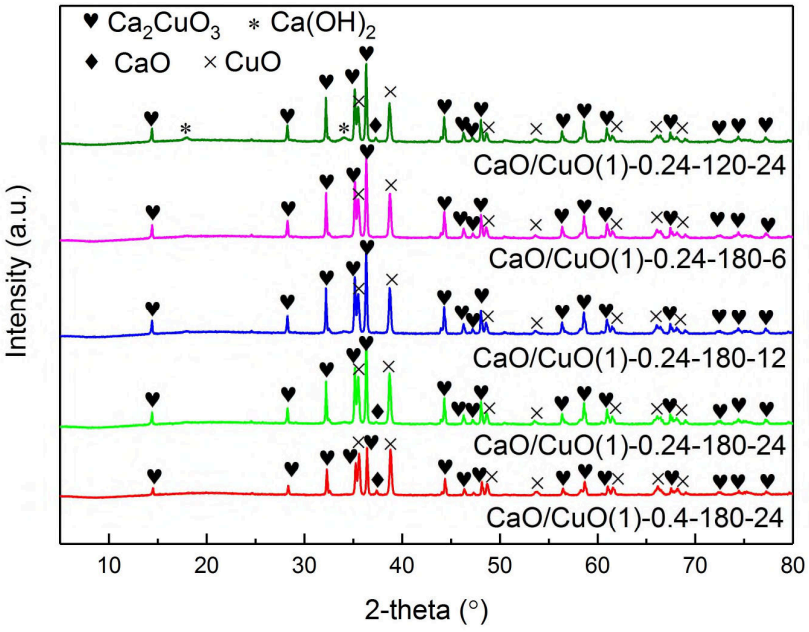

Figure 6. XRD diffractograms of CaO/CuO composites prepared by the template-free synthesis method under different hydrothermal conditions.

Assessment of carbonation and redox characteristics of CaO/CuO hollow microspheres. Compared to CaO/CuO composites prepared via the conventional synthesis methods, an entirely different structure, i.e., CaO/CuO hollow microspheres featuring highly porous shells and homogeneous elemental distribution, was obtained in this work. To the best of our knowledge, this unique structure is being reported for the first time in material synthesis for the combined Ca-Cu looping process. As the structure of the sorbents plays a critical role for high sorption capacities [1][2],[53,54] the carbonation and redox characteristics of CaO/CuO hollow microspheres should be investigated in detail.

It is well known that the reaction conditions also have significant effect on the sorption capacity of CaO-based sorbents.[55-58] Thus, we first explored the effect of reaction conditions on the carbonation and redox characteristics of CaO/CuO hollow microspheres. Figure 7 gives typical carbonation and oxidation curves of CaO/CuO(1)-0.4-180-24 under different carbonation and oxidation temperatures, respectively. It was found the carbonation temperature played a critical role in CO_2 uptake capacity. As the carbonation temperature increased, the CO_2 uptake increased first, reaching a maximum carbonation conversion of 59.5% at 650 °C, and then it decreased to 47.1% at 700 °C (Figure 7a). However, it seemed the oxidation temperature had a negligible effect on the O_2 carrying capacity. With the increase of oxidation temperature, there were no obvious changes in the measured O_2 carrying capacity, and the oxidation was always fast with conversions larger than 90% (Figure 7b).

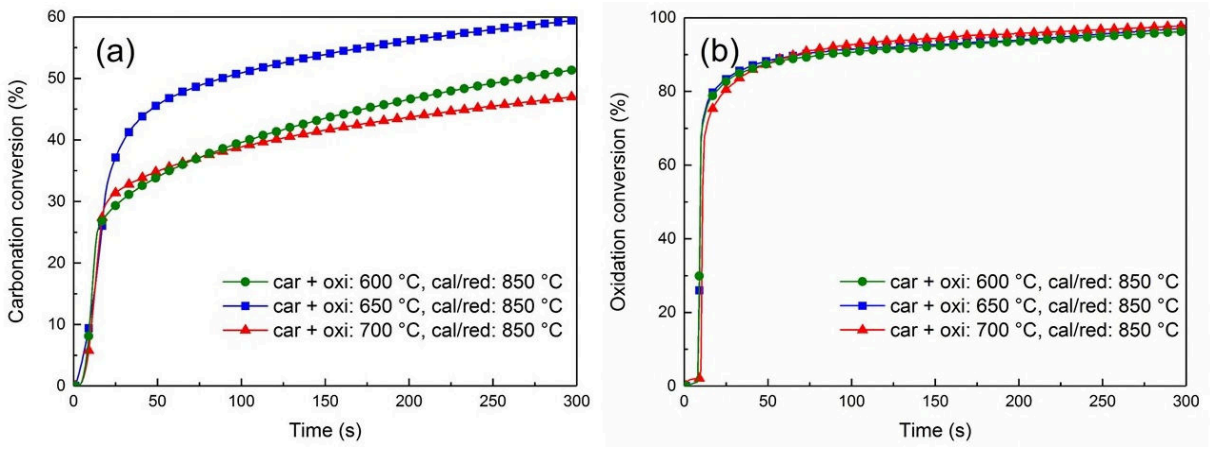

Figure 7. (a) Carbonation and (b) oxidation curves of CaO/CuO hollow microspheres (CaO/CuO(1)-0.4-180-24) during the initial carbonation and oxidation stages in a fixed-bed reactor, respectively.

Figure 8 gives carbonation and redox characteristics of CaO/CuO hollow microspheres over the tested cycles. CaO/CuO(1)-0.4-180-24 exhibited a slightly lower carbonation conversion than CaO/CuO(1)-0.24-180-24 (i.e., 59.5% vs. 65.5%), and the transition point of CaO/CuO(1)-0.4-180-24 (i.e., from the kinetically-controlled stage to the diffusion-controlled stage of the carbonation reaction) was present later than that of CaO/CuO(1)-0.24-180-24. This was due to the higher CO_2 diffusion resistance resulting from the increased shell thickness of the microspheres (as shown in Figure 5 and SI, Figure S2). More importantly, CaO/CuO(1)-0.24-180-24 possessed an initial carbonation conversion of 65.5% within a carbonation duration of 5 min, whereas a carbonation conversion value of 51.9% was obtained within the first minute, contributing to 79.2% of the initial CO_2 uptake capacity. This result suggests that the CaO/CuO hollow microspheres possessed good CO_2 sorption kinetics, which is important given the rather short residence times in a real process. After ten repeated cycles, the carbonation conversion of CaO/CuO(1)-0.24-180-24 declined to 45.4%, still retaining 69.3% of its initial CO_2 uptake capacity (Figure 8b). An

261 additional test covering 20 cycles was conducted for the best material, i.e., CaO/CuO(1)-0.24-180-
262 24. From cycle number eight onwards, the CO_2 uptake was very stable (Figure 8a), implying the
263 good cyclic stability of the CaO/CuO hollow microspheres. In terms of O_2 carrying capacity,
264 CaO/CuO hollow microspheres possessed excellent, cyclically stable O_2 carrying capacity (Figure
265 8c, d), as has often been observed in previous work.[11,25]

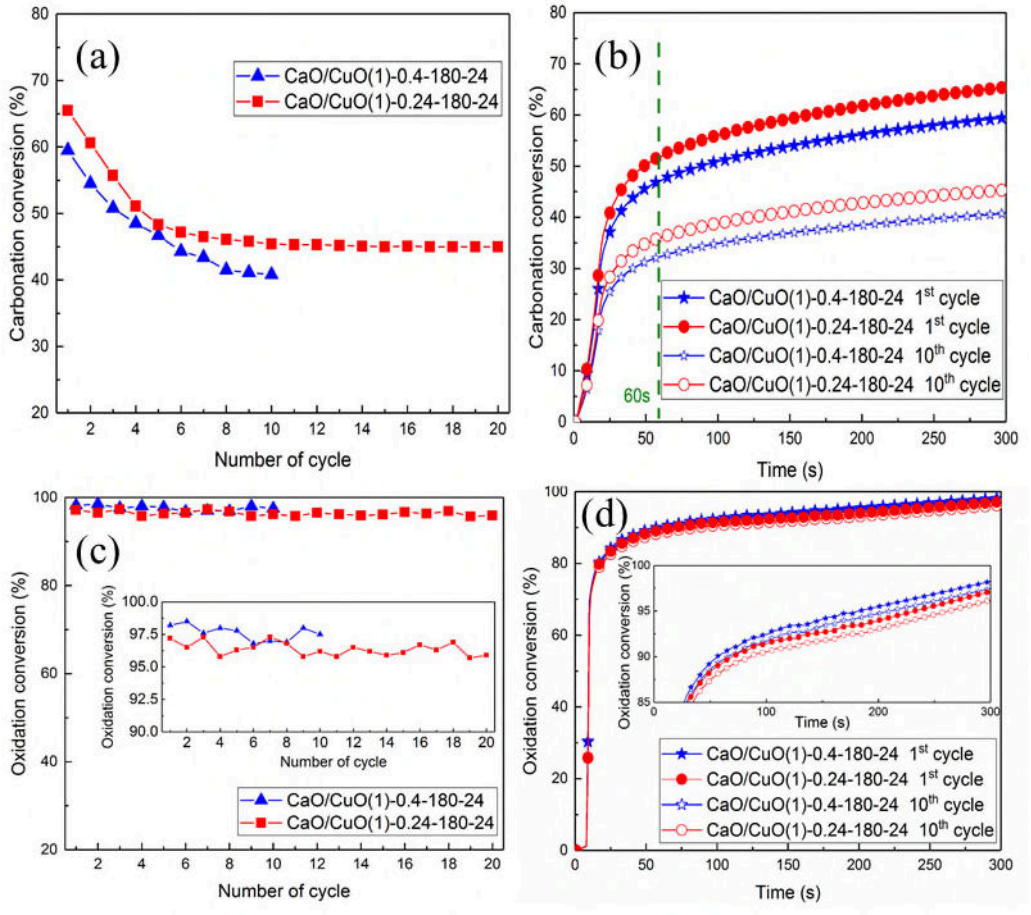

266

267 **Figure 8.** Carbonation and redox characteristics of CaO/CuO hollow microspheres in a fixed-
268 bed reactor. (a) Carbonation conversion as a function of cycle number; (b) Corresponding
269 carbonation curves in the first and 10th cycle (the vertical dashed line corresponds to a
270 carbonation time of 60 s.); (c) Oxidation conversion as a function of cycle number; (d)

Corresponding oxidation curves in the first and 10th cycle. Reaction condition: calcination/reduction stage: 20 vol.% CH_4 (N_2 bal.), 850 °C, 10 min; oxidation stage: 21 vol.% O_2 (N_2 bal.), 650 °C, 5 min; carbonation stage: 15 vol.% CO_2 (N_2 bal.), 650 °C, 5 min.

In a real process the objective is to capture CO_2 during carbonation and generate a pure stream of CO_2 suitable for sequestration in the calcination process step. To achieve this, thermodynamics for the system CaO-$CaCO_3$ dictate that the temperature in the calcination reactor must be greater than ~ 900 °C (assuming an atmosphere containing 100% CO_2 at 1 atmosphere).[56] Under these harsh conditions, the CO_2 uptake capacity decreases much more rapidly than under mild conditions, where the calcination is performed at lower temperatures in an environment free of CO_2. We, therefore, ran experiments under extremely harsh conditions (i.e., the calcination/reduction reaction was performed for 10 min at 940 °C in an atmosphere of 20 vol.% CH_4 (CO_2 balance)), aiming to emulate a real process as closely as possible and thus assess the real carbonation and redox characteristics of the materials. As shown in the SI, Figure S7, CaO/CuO hollow microspheres (CaO/CuO(1)-0.24-180-24) still possessed a carbonation conversion of 60.1% initially, and 37.5% after ten repeated cycles, whereas the oxidation conversion was always larger than 89%. These results confirmed that CaO/CuO hollow microspheres still exhibited good CO_2 capture performance and excellent redox characteristics.

Structure-performance relationship of the CaO/CuO composites tested. Figure 9 compares the carbonation and redox performance of CaO/CuO composites fabricated by different synthesis methods over ten repeated cycles. The decline in CO_2 uptake capacity of CaO/CuO composites was observed for all samples; however, it was clear that CaO/CuO hollow microspheres exhibited significantly enhanced CO_2 capture performance compared to CaO/CuO composites fabricated by wet mixing and co-precipitation methods (Figure 9a). As shown in the SI, Table S2, the initial

carbonation conversion of CaO/CuO(1)-0.24-180-24 was 65.5%, exceeding that of CaO/CuO(1)-0.24-WM by 44.3% and that of CaO/CuO(1)-0.24-CP by 24.3%, respectively. After ten repeated cycles, the final carbonation conversion of CaO/CuO(1)-0.24-180-24 was 45.4%, exceeding that of CaO/CuO(1)-0.24-WM by 222% and CaO/CuO(1)-0.24-CP by 114%, respectively. Moreover, the decline in CO_2 capture performance was significantly suppressed by CaO/CuO hollow microspheres. The decline rate in CO_2 uptake capacity for CaO/CuO composites prepared by wet mixing or co-precipitation was larger than 60% over the ten repeated cycles. However, CaO/CuO hollow microspheres still maintained approximately 60% of their initial CO_2 uptake capacity. Furthermore, although different synthesis methods were used to fabricate CaO/CuO composites, the oxidation conversions of all the composites were greater than 90% over the ten repeated cycles (Figure 9b). This result suggested the excellent redox characteristics of CaO/CuO composites, irrespective of the synthesis method used.

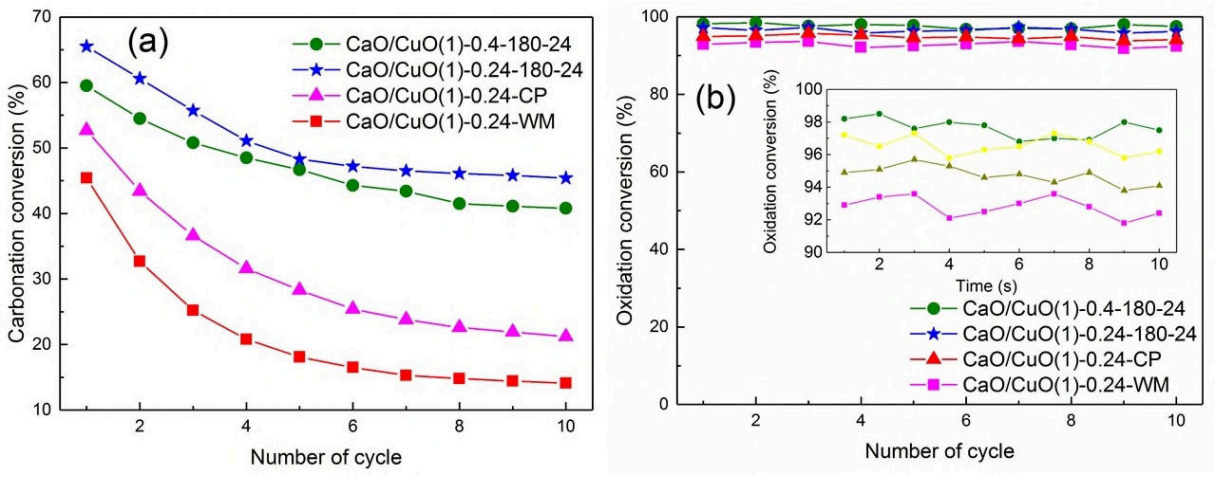

Figure 9. (a) Carbonation conversion and (b) oxidation conversion of CaO/CuO composites prepared by different synthesis methods over the tested cycles in a fixed-bed reactor, respectively. Reaction condition: calcination/reduction stage: 20 vol.% CH_4 (N_2 bal.), 850 °C, 10 min; oxidation stage: 21 vol.% O_2 (N_2 bal.), 650 °C, 5 min; carbonation stage: 15 vol.% CO_2

311 (N_2 bal.), 650 °C, 5 min.

312 Figure 10 and Figure 11 show SEM images of the CaO/CuO composites prepared by different
313 methods when they were collected at different stages of the repeated calcination/reduction,
314 oxidation, and carbonation cycles, respectively. Hollow microsphere structures featuring highly
315 porous shells were obtained only when the template-free synthesis approach was used, whereas
316 irregular morphologies were obtained when wet mixing or co-precipitation methods were used. It
317 can be seen that the shells of CaO/CuO hollow microspheres possessed an appreciable degree of
318 porosity even in their carbonated state (Figure 10b). Moreover, CaO/CuO hollow microspheres
319 still retained their hollow microsphere structures with porous shells, despite undergoing ten
320 repeated cycles (Figure 10d, Figure 11b, SI, Figure S8 and SI, Figure S9). However, CaO/CuO
321 composites fabricated by wet mixing or co-precipitation methods exhibited greater changes in their
322 morphologies after ten repeated cycles. Significant agglomeration is observed in Figure 11d, f,
323 mainly due to the lack of well-defined structures; i.e., hollow microsphere structures featuring
324 highly porous shells, which enabled a physical separation of the nanoparticles and, thus, mitigated
325 particle/grain agglomeration effectively.[44]

326 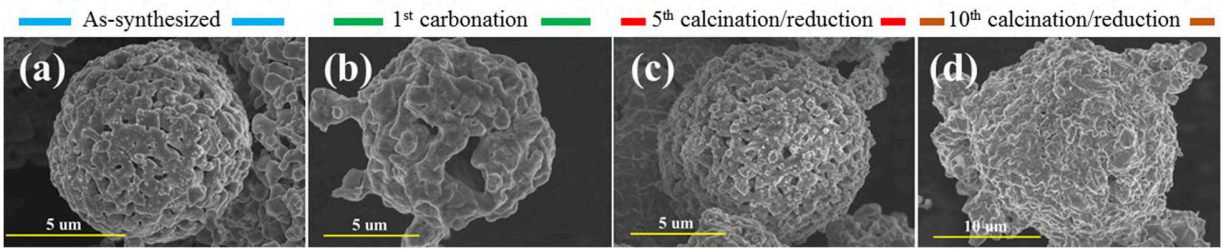

327 **Figure 10.** Morphological changes of CaO/CuO(1)-0.24-180-24 at different stages of repeated
328 calcination/reduction, oxidation and carbonation cycles. Reaction conditions:

calcination/reduction stage: 20 vol.% CH_4 (N_2 bal.), 850 °C, 10 min; oxidation stage: 21 vol.% O_2 (N_2 bal.), 650 °C, 5 min; carbonation stage: 15 vol.% CO_2 (N_2 bal.), 650 °C, 5 min.

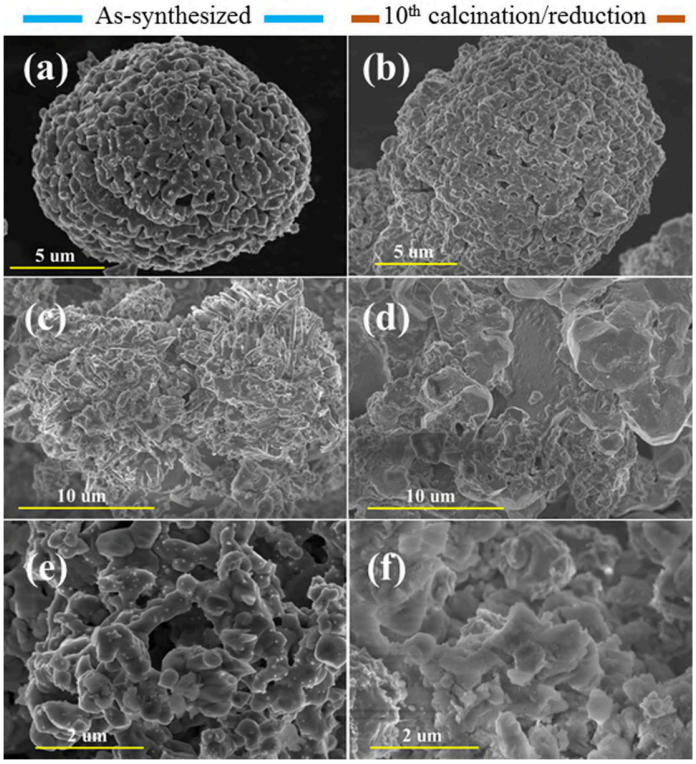

Figure 11. Morphological changes of CaO/CuO composites prepared by different synthesis methods at different stages of repeated cycles. (a), (b) CaO/CuO(1)-0.4-180-24; (c), (d) CaO/CuO(1)-0.24-WM; (e), (f) CaO/CuO(1)-0.24-CP. Reaction conditions: calcination/reduction stage: 20 vol.% CH_4 (N_2 bal.), 850 °C, 10 min; oxidation stage: 21 vol.% O_2 (N_2 bal.), 650 °C, 5 min; carbonation stage: 15 vol.% CO_2 (N_2 bal.), 650 °C, 5 min.

In order to shed light on the structure-performance relationship of the materials, specific surface area and pore volume were measured using N_2 adsorption (Table 1 and SI, Figure S10). CaO/CuO hollow microspheres possessed higher surface areas and pore volumes than the CaO/CuO composites prepared by wet mixing or co-precipitation methods, which can be ascribed to the

inherent advantages of well-defined structures, i.e., hollow microsphere structures featuring highly porous shells. After ten repeated cycles, there were substantial drops in both surface area and pore volume for all the CaO/CuO composites due to the thermal sintering. However, CaO/CuO hollow microspheres still possessed higher surface areas than the reference materials, as the well-defined structures were largely retained after the repeated cycles (as shown in Figure 10, Figure 11, SI, Figure S8 and SI, Figure S9). The surface areas of the CaO/CuO composites decreased in the following order: CaO/CuO(1)-0.24-180-24 > CaO/CuO(1)-0.4-180-24 > CaO/CuO(1)-0.24-CP > CaO/CuO(1)-0.24-WM, which was in agreement with their cyclic CO_2 capture performance. In terms of pore volume of the composites after ten cycles, CaO/CuO(1)-0.24-180-24 possessed the highest while CaO/CuO(1)-0.24-WM possessed the lowest. CaO/CuO(1)-0.4-180-24 and CaO/CuO(1)-0.24-CP possessed roughly the same pore volume after cyclic operations, although the former exhibited a much better CO_2 capture performance than the latter. In light of these observations, it can be concluded that both the hollow microsphere structures and the highly porous shells were essential characteristics to maintain cyclically high CO_2 capture performance of CaO/CuO composites.

Table 1. Porosity characterizations of CaO/CuO composites before and after repeated cycles

Sample	As-synthesized		After ten cycles (calcined/reduced state)	
	Surface area (m^2/g)	Pore volume (cm^3/g)	Surface area (m^2/g)	Pore volume (cm^3/g)
CaO/CuO(1)-0.24-CP	16.7	0.027	4.6	0.019
CaO/CuO(1)-0.24-WM	14.7	0.023	2.1	0.013

CaO/CuO(1)-0.24-180-24	33.9	0.031	7.8	0.024
CaO/CuO(1)-0.4-180-24	24.0	0.043	6.6	0.019

Further, the phase evolutions of the CaO/CuO hollow microspheres during the calcination/reduction, oxidation and carbonation cycles were investigated by XRD (Figure S11). As mentioned above, the main components of the as-synthesized CaO/CuO(1)-0.4-180-24 were CaO, CuO and Ca_2CuO_3. However, only CaO and Cu were detected after the first calcination/reduction reaction, indicating Ca_2CuO_3 decomposed to CaO and Cu and was thus an active component for the combined Ca-Cu looping.[23,25] Moreover, Cu was not detected and only CuO and CaO were present after the subsequent oxidation reaction, indicating the complete oxidation of Cu. After the carbonation reaction, $CaCO_3$ was present, which confirmed the occurrence of the carbonation reaction between CaO and CO_2. However, CaO, together with CuO, was still present, indicating the incomplete carbonation of CaO/CuO hollow microspheres, in agreement with the results from the fixed-bed experiments. Hence, it can be concluded that there were no side reactions between $CaO/CaCO_3$ and CuO/Cu during the combined Ca-Cu looping process, which was of great importance for this promising technology.

ASSOCIATED CONTENT

Supporting Information.

This information is available free of charge via the Internet at http://pubs.acs.org.

Experimental characterization; experimental performance test; schematic illustration of bench-scale fixed-bed reactor; morphology of CaO/CuO(1)-0.4-180-24 and CaO/CuO(1)-0.24-120-24; SEM images of CaO/CuO composites synthesized without hydrothermal treatment or with the

absence of glycine; SEM-EDX mappings of CaO/CuO(1)-0.24-180-24; comparison of carbonation and redox characteristics of CaO/CuO(1)-0.24-180-24 under different reaction conditions; TEM image of CaO/CuO(1)-0.24-180-24 after five repeated cycles; SEM images of broken CaO/CuO(1)-0.24-180-24 after ten repeated cycles; pore size distributions of CaO/CuO composites before and after the repeated cycles; XRD diffractograms of CaO/CuO hollow microspheres (CaO/CuO(1)-0.4-180-24) during repeated calcination/reduction, oxidation and carbonation cycles; CO_2 capture performance of CaO/CuO composites prepared by different synthesis methods.

AUTHOR INFORMATION

Corresponding Author

*E-mail: duanlunbo@seu.edu.cn

Author Contributions

The manuscript was written through contributions of all authors. All authors have given approval to the final version of the manuscript.

Notes

The authors declare no competing financial interest.

ACKNOWLEDGMENT

We acknowledge the financial support from the National Key Research and Development Program of China (2016YFE0102500-06-01), Scientific Research Foundation of Graduate School

of Southeast University, China (YBPY1902), and the Program of China Scholarships Council (No. 201806090031).

REFERENCES

(1) Su, C.; Duan, L.; Donat, F.; Anthony, E. J. From Waste to High Value Utilization of Spent Bleaching Clay in Synthesizing High-Performance Calcium-Based Sorbent for CO_2 Capture. *Appl. Energy* **2018**, *210*, 117–126.

(2) Xu, Y.; Ding, H.; Luo, C.; Zheng, Y.; Xu, Y.; Li, X.; Zhang, Z.; Shen, C.; Zhang, L. Effect of Lignin, Cellulose and Hemicellulose on Calcium Looping Behavior of CaO-Based Sorbents Derived from Extrusion-Spherization Method. *Chem. Eng. J.* **2018**, *334*, 2520–2529.

(3) Donat, F.; Florin, N. H.; Anthony, E. J.; Fennell, P. S. Influence of High-Temperature Steam on the Reactivity of CaO Sorbent for CO_2 Capture. *Environ. Sci. Technol.* **2012**, *46* (2), 1262–1269.

(4) Filitz, R.; Kierzkowska, A.; Broda, M.; Mueller, C. R. Highly Efficient CO_2 Sorbents: Development of Synthetic, Calcium-Rich Dolomites. *Environ. Sci. Technol.* **2012**, *46* (1), 559–565.

(5) Qin, C.; He, D.; Zhang, Z.; Tan, L.; Ran, J. The Consecutive Calcination/Sulfation in Calcium Looping for CO_2 Capture: Particle Modeling and Behaviour Investigation. *Chem. Eng. J.* **2018**, *334*, 2238–2249.

(6) Xu, Y.; Ding, H.; Luo, C.; Zheng, Y.; Zhang, Q.; Li, X.; Sun, J.; Zhang, L. Potential Synergy of Chlorine and Potassium and Sodium Elements in Carbonation Enhancement of CaO-Based Sorbents. *ACS Sustain. Chem. Eng.* **2018**, *6* (9), 11677–11684.

(7) Abanades, J. C.; Murillo, R.; Fernandez, J. R.; Grasa, G.; Martínez, I. New CO_2 Capture Process for Hydrogen Production Combining Ca and Cu Chemical Loops. *Environ. Sci. Technol.* **2010**, *44* (17), 6901–6904.

(8) Fernández, J. R.; Abanades, J. C. Overview of the Ca–Cu Looping Process for Hydrogen Production and/or Power Generation. *Curr. Opin. Chem. Eng.* **2017**, *17*, 1–8.

(9) Manovic, V.; Anthony, E. J. Integration of Calcium and Chemical Looping Combustion Using Composite CaO/CuO-Based Materials. *Environ. Sci. Technol.* **2011**, *45* (24), 10750–10756.

(10) Qin, C.; Yin, J.; Feng, B.; Ran, J.; Zhang, L.; Manovic, V. Modelling of the Calcination Behaviour of a Uniformly-Distributed CuO/$CaCO_3$ Particle in Ca-Cu Chemical Looping. *Appl. Energy* **2016**, *164*, 400–410.

(11) Duan, L.; Godino, D.; Manovic, V.; Montagnaro, F.; Anthony, E. J. Cyclic Oxygen Release Characteristics of Bifunctional Copper Oxide/Calcium Oxide Composites. *Energy Technol.* **2016**, *4* (10), 1171–1178.

(12) Arias, B.; Diego, M. E.; Méndez, A.; Alonso, M.; Abanades, J. C. Calcium Looping Performance under Extreme Oxy-Fuel Combustion Conditions in the Calciner. *Fuel* **2018**, *222*, 711–717.

(13) Ozcan, D. C.; Macchi, A.; Lu, D. Y.; Kierzkowska, A. M.; Ahn, H.; Müller, C. R.; Brandani, S. Ca-Cu Looping Process for CO_2 Capture from a Power Plant and Its Comparison with Ca-Looping, Oxy-Combustion and Amine-Based CO_2 Capture Processes. *Int. J. Greenh. Gas Control* **2015**, *43*, 198–212.

(14) Martínez, I.; Romano, M. C.; Fernández, J. R.; Chiesa, P.; Murillo, R.; Abanades, J. C. Process Design of a Hydrogen Production Plant from Natural Gas with CO_2 Capture Based on a Novel Ca/Cu Chemical Loop. *Appl. Energy* **2014**, *114*, 192–208.

(15) Martini, M.; van den Berg, A.; Gallucci, F.; van Sint Annaland, M. Investigation of the Process Operability Windows for Ca-Cu Looping for Hydrogen Production with CO_2 Capture. *Chem. Eng. J.* **2016**, *303*, 73–88.

(16) Riva, L.; Martínez, I.; Martini, M.; Gallucci, F.; van Sint Annaland, M.; Romano, M. C. Techno-Economic Analysis of the Ca-Cu Process Integrated in Hydrogen Plants with CO_2 Capture. *Int. J. Hydrogen Energy* **2018**, *43* (33), 15720–15738.

(17) Fernández, J. R.; Abanades, J. C. Optimized Design and Operation Strategy of a Ca-Cu Chemical Looping Process for Hydrogen Production. *Chem. Eng. Sci.* **2017**, 1–36.

(18) Martínez, I.; Armaroli, D.; Gazzani, M.; Romano, M. C. Integration of the Ca-Cu Process in Ammonia Production Plants. *Ind. Eng. Chem. Res.* **2017**, *56* (9), 2526–2539.

(19) Martínez, I.; Murillo, R.; Grasa, G.; Fernández, J. R.; Abanades, J. C. Integrated Combined Cycle from Natural Gas with CO_2 Capture Using a Ca-Cu Chemical Loop. *AIChE J.* **2013**, *59* (8), 2780–2794.

(20) Fernández, J. R.; Martínez, I.; Abanades, J. C.; Romano, M. C. Conceptual Design of a Ca–Cu Chemical Looping Process for Hydrogen Production in Integrated Steelworks. *Int. J. Hydrogen Energy* **2017**, 1–15.

(21) Martínez, I.; Fernández, J. R.; Abanades, J. C.; Romano, M. C. Integration of a Fluidised Bed Ca–Cu Chemical Looping Process in a Steel Mill. *Energy* **2018**, *163*, 570–584.

(22) Diglio, G.; Bareschino, P.; Mancusi, E.; Pepe, F.; Montagnaro, F.; Hanak, D. P.; Manovic, V. Feasibility of CaO/CuO/NiO Sorption-Enhanced Steam Methane Reforming Integrated with Solid-Oxide Fuel Cell for Near-Zero-CO_2 Emissions Cogeneration System. *Appl. Energy* **2018**, *230*, 241–256.

462 (23) Chen, J.; Duan, L.; Donat, F.; Müller, C. R.; Anthony, E. J.; Fan, M. Self-Activated ,
463 Nanostructured Composite for Improved CaL-CLC Technology. *Chem. Eng. J.* **2018**, *351*, 1038–
464 1046.
465 (24) Qin, C.; Yin, J.; Liu, W.; An, H.; Feng, B. Behavior of CaO/CuO Based Composite in a
466 Combined Calcium and Copper Chemical Looping Process. *Ind. Eng. Chem. Res.* **2012**, *51* (38),
467 12274–12281.
468 (25) Kierzkowska, A. M.; Müller, C. R. Development of Calcium-Based, Copper-Functionalised
469 CO_2 Sorbents to Integrate Chemical Looping Combustion into Calcium Looping. *Energy Environ.*
470 *Sci.* **2012**, *5* (3), 6061–6065.
471 (26) Kierzkowska, A. M.; Müller, C. R. Sol-Gel-Derived, Calcium-Based, Copper-Functionalised
472 CO_2 Sorbents for an Integrated Chemical Looping Combustion-Calcium Looping CO_2 Capture
473 Process. *Chempluschem* **2013**, *78* (1), 92–100.
474 (27) Manovic, V.; Wu, Y.; He, I.; Anthony, E. J. Core-in-Shell CaO/CuO-Based Composite for
475 CO_2 Capture. *Ind. Eng. Chem. Res.* **2011**, *50* (22), 12384–12391.
476 (28) Wang, B.; Wu, H.; Yu, L.; Xu, R.; Lim, T. T.; Lou, X. W. Template-Free Formation of
477 Uniform Urchin-like α-FeOOH Hollow Spheres with Superior Capability for Water Treatment.
478 *Adv. Mater.* **2012**, *24* (8), 1111–1116.
479 (29) Guo, H.; Wang, Y.; Wang, W.; Liu, L.; Guo, Y.; Yang, X.; Wang, S. Template-Free
480 Fabrication of Hollow NiO-Carbon Hybrid Nanoparticle Aggregates with Improved Lithium
481 Storage. *Part. Part. Syst. Charact.* **2014**, *31* (3), 374–381.
482 (30) Tian, Z.; Zhou, Y.; Li, Z.; Liu, Q.; Zou, Z. Generalized Synthesis of a Family of Multishelled
483 Metal Oxide Hollow Microspheres. *J. Mater. Chem. A* **2013**, *1* (11), 3575–3579.

(31) Guan, J.; Mou, F.; Sun, Z.; Shi, W. Preparation of Hollow Spheres with Controllable Interior Structures by Heterogeneous Contraction. *Chem. Commun.* **2010**, *46* (35), 6605–6607.

(32) Yu, L.; Hu, H.; Wu, H. Bin; Lou, X. W. D. Complex Hollow Nanostructures: Synthesis and Energy-Related Applications. *Adv. Mater.* **2017**, *29* (15).

(33) Li, Y.; Shi, J. Hollow-Structured Mesoporous Materials: Chemical Synthesis, Functionalization and Applications. *Adv. Mater.* **2014**, *26* (20), 3176–3205.

(34) Zhou, L.; Zhuang, Z.; Zhao, H.; Lin, M.; Zhao, D.; Mai, L. Intricate Hollow Structures: Controlled Synthesis and Applications in Energy Storage and Conversion. *Adv. Mater.* **2017**, *29* (20).

(35) Derevschikov, V.; Semeykina, V.; Bitar, J.; Parkhomchuk, E.; Okunev, A. Template Technique for Synthesis of CaO-Based Sorbents with Designed Macroporous Structure. *Microporous Mesoporous Mater.* **2017**, *238*, 56–61.

(36) Chen, J.; Duan, L.; Sun, Z. Accurate Control of Cage-Like CaO Hollow Microspheres for Enhanced CO_2 Capture in Calcium Looping via a Template-Assisted Synthesis Approach. *Environ. Sci. Technol.* **2019**, *53* (4), 2249–2259.

(37) Broda, M.; Manovic, V.; Anthony, E. J.; Müller, C. R. Effect of Pelletization and Addition of Steam on the Cyclic Performance of Carbon-Templated, CaO-Based CO_2 Sorbents. *Environ. Sci. Technol.* **2014**, *48* (9), 5322–5328.

(38) Ma, X.; Li, Y.; Duan, L.; Anthony, E.; Liu, H. CO_2 Capture Performance of Calcium-Based Synthetic Sorbent with Hollow Core-Shell Structure under Calcium Looping Conditions. *Appl. Energy* **2018**, *225*, 402–412.

505 (39) Armutlulu, A.; Naeem, M. A.; Liu, H.-J.; Kim, S. M.; Kierzkowska, A.; Fedorov, A.; Müller,
506 C. R. Multishelled CaO Microspheres Stabilized by Atomic Layer Deposition of Al_2O_3 for
507 Enhanced CO_2 Capture Performance. *Adv. Mater.* **2017**, *29* (41), 1702896.
508 (40) Yan, F.; Jiang, J.; Li, K.; Liu, N.; Chen, X.; Gao, Y.; Tian, S. Green Synthesis of Nanosilica
509 from Coal Fly Ash and Its Stabilizing Effect on CaO Sorbents for CO_2 Capture. *Environ. Sci.*
510 *Technol.* **2017**, *51* (13), 7606–7615.
511 (41) Peng, W.; Xu, Z.; Luo, C.; Zhao, H. Tailor-Made Core–Shell CaO/TiO_2–Al_2O_3 Architecture
512 as a High-Capacity and Long-Life CO_2 Sorbent. *Environ. Sci. Technol.* **2015**, *49* (13), 8237–8245.
513 (42) Tian, S.; Jiang, J.; Yan, F.; Li, K.; Chen, X. Synthesis of Highly Efficient CaO-Based, Self-
514 Stabilizing CO_2 Sorbents via Structure-Reforming of Steel Slag. *Environ. Sci. Technol.* **2015**, *49*
515 (12), 7464–7472.
516 (43) Wang, S.; Fan, S.; Fan, L.; Zhao, Y.; Ma, X. Effect of Cerium Oxide Doping on the
517 Performance of CaO-Based Sorbents during Calcium Looping Cycles. *Environ. Sci. Technol.*
518 **2015**, *49* (8), 5021–5027.
519 (44) Naeem, M. A.; Armutlulu, A.; Imtiaz, Q.; Donat, F.; Schäublin, R.; Kierzkowska, A.; Müller,
520 C. R. Optimization of the Structural Characteristics of CaO and Its Effective Stabilization Yield
521 High-Capacity CO_2 Sorbents. *Nat. Commun.* **2018**, *9* (1), 1–11.
522 (45) Broda, M.; Kierzkowska, A. M.; Müller, C. R. Development of Highly Effective CaO-Based,
523 MgO-Stabilized CO_2 Sorbents via a Scalable "One-Pot" Recrystallization Technique. *Adv. Funct.*
524 *Mater.* **2014**, *24* (36), 5753–5761.
525 (46) Ping, H.; Wu, S. Preparation of Cage-like Nano-$CaCO_3$ Hollow Spheres for Enhanced CO_2
526 Sorption. *RSC Adv.* **2015**, *5* (80), 65052–65057.

(47) Wang, J.; Huang, L.; Yang, R.; Zhang, Z.; Wu, J.; Gao, Y.; Wang, Q.; O'Hare, D.; Zhong, Z. Recent Advances in Solid Sorbents for CO_2 Capture and New Development Trends. *Energy Environ. Sci.* **2014**, *7* (11), 3478–3518.

(48) Liu, F.-Q.; Li, W.-H.; Liu, B.-C.; Li, R.-X. Synthesis, Characterization, and High Temperature CO_2 Capture of New CaO Based Hollow Sphere Sorbents. *J. Mater. Chem. A* **2013**, *1* (27), 8037.

(49) Naeem, M. A.; Armutlulu, A.; Broda, M.; Lebedev, D.; Müller, C. R. The Development of Effective CaO-Based CO_2 sorbents: Via a Sacrificial Templating Technique. *Faraday Discuss.* **2016**, *192*, 85–95.

(50) Mosaddegh, E.; Hassankhani, A. Preparation, Characterization, and Catalytic Activity of Ca_2CuO_3/$CaCu_2O_3$/CaO Nanocomposite as a Novel and Bio-Derived Mixed Metal Oxide Catalyst in the Green Synthesis of 2H-Indazolo[2,1-b]Phthalazine-Triones. *Catal. Commun.* **2015**, *71*, 65–69.

(51) Huynh, D.-C.; Ngo, D.-T.; Hoang, N.-N. Structure and Electrical Properties of the Spin 1/2 One-Dimensional Antiferromagnet Ca_2CuO_3 Prepared by the Sol–gel Technique. *J. Phys. Condens. Matter* **2007**, *19* (10), 106215.

(52) Lin, S.; Wang, Y.; Suzuki, Y. High-Temperature CaO Hydration/$Ca(OH)_2$ Decomposition over a Multitude of Cycles. *Energy and Fuels* **2009**, *23* (6), 2855–2861.

(53) Imtiaz, Q.; Broda, M.; Müller, C. R. Structure-Property Relationship of Co-Precipitated Cu-Rich, Al_2O_3- or $MgAl_2O_4$-Stabilized Oxygen Carriers for Chemical Looping with Oxygen Uncoupling (CLOU). *Appl. Energy* **2014**, *119*, 557–565.

(54) Harvey, O. R.; Herbert, B. E.; Rhue, R. D.; Kuo, L.-J. Metal Interactions at the Biochar-Water Interface: Energetics and Structure-Sorption Relationships Elucidated by Flow Adsorption Microcalorimetry. *Environ. Sci. Technol.* **2011**, *45* (13), 5550–5556.

(55) Criado, Y. A.; Arias, B.; Abanades, J. C. Effect of the Carbonation Temperature on the CO_2 Carrying Capacity of CaO. *Ind. Eng. Chem. Res.* **2018**, *57* (37), 12595–12599.

(56) Kierzkowska, A. M.; Pacciani, R.; Müller, C. R. CaO-Based CO_2 Sorbents: From Fundamentals to the Development of New, Highly Effective Materials. *ChemSusChem* **2013**, *6* (7), 1130–1148.

(57) Broda, M.; Kierzkowska, A. M.; Müller, C. R. Influence of the Calcination and Carbonation Conditions on the CO_2 uptake of Synthetic Ca-Based CO_2 Sorbents. *Environ. Sci. Technol.* **2012**, *46* (19), 10849–10856.

(58) Donat, F.; Müller, C. R. A Critical Assessment of the Testing Conditions of CaO-Based CO_2 Sorbents. *Chem. Eng. J.* **2018**, *336*, 544–549.